Plant, Cell & Environment

Plant, Cell and Environment (2010) **33**, 1234–1238 doi: 10.1111/j.1365-3040.2010.02142.x

A computational algorithm addressing how vessel length might depend on vessel diameter

JING CAI[1,2], SHUOXIN ZHANG[1] & MELVIN T. TYREE[2,3]

[1]College of Forestry, Northwest A&F University, Yangling, Shaanxi, 712100, China, [2]Department of Renewable Resources, University of Alberta, Edmonton, AB, Canada, T6G 2E3 and [3]United States Forest Service, Northern Research Station, S. Burlington, VT 05403, USA

ABSTRACT

The objective of this method paper was to examine a computational algorithm that may reveal how vessel length might depend on vessel diameter within any given stem or species. The computational method requires the assumption that vessels remain approximately constant in diameter over their entire length. When this method is applied to three species or hybrids in the genus *Populus*, vessel length is sometimes a linear function of vessel diameter and sometimes an exponential function of vessel diameter within a stem, based on R^2 values. Our results give within-species variation of vessel length versus diameter, and we compare this to between-species variation of mean diameter versus mean length.

Key-words: aspen; cottonwood hybrids Northwest and P38P38; vessel diameter; vessel length; Weibull functions.

Abbreviations: A, vessel cross-sectional area; D, vessel diameter; $\bar{D}_v$, mean vessel diameter in a stem; d_w, bin diameter width; k, Weibull probability density function (PDF) constant Eqn 1; L_c, vessel length in a bin diameter size class; $\bar{L}_c$, mean vessel length in a stem; N, number of rubber-filled vessels per unit area; N_c, number of rubber-filled vessels per unit area in a bin diameter size class; N_o, number of rubber-filled vessels per unit area at 2 mm from injection surface; P_x, probability of vessels in length interval dx; x, distance from infusion surface (rubber or paint); x_b, bin diameter increment = D_c/d_w; λ, Weibull PDF constant Eqn 1; λ_c, exponential coefficient in Eqn 2.

INTRODUCTION

Skene & Balodis (1968) provided the first rigorous treatment of vessel length distribution, although a few older papers talk about maximum vessel length (Grenidge 1952) or 'average' vessel length (Scholander 1958). A cinematographic technique used by Zimmermann (1971, 1978) provides accurate vessel length distributions, but is too labour intensive for general use. Hence, the preferred approach is to: (1) visualize the length of cut-open vessels measured from the cut surface of a stem by injecting with some easily observed substance; and (2) use a computational algorithm to deduce vessel length distributions based on a few assumptions (Zimmermann & Jeje 1981; Ewers & Fisher 1989; Tyree 1993). Vessel lengths can be evaluated in any plant axis (stem, root or petiole).

The accurate evaluation of vessel lengths (or vessel length distributions) has attracted increased interest, because vessel size has influence on vessel vulnerability to cavitation (e.g. Wheeler *et al*. 2005). In addition, conduit length is a consideration in theories about optimization of conduit structure for hydraulic efficiency (e.g. Lancashire & Ennos 2002; Wheeler *et al*. 2005), and is used in hydraulic models (e.g. Loepfe *et al*. 2007).

When examining mean vessel lengths ($\bar{L}_v$) among species, $\bar{L}_v$ seems to increase with mean vessel diameter ($\bar{D}_v$), for example Ewers, Fisher & Chiu (1990) reported that the maximum vessel diameter correlated linearly with maximum vessel length among species of woody vines and shrubs ($R^2 = 0.62$; $P = 0.001$). Hacke *et al*. (2006) have summarized between-species values (28 species) of $\bar{L}_v$ and $\bar{D}_v$, and showed that a plot of log($\bar{L}_v$) versus log ($\bar{D}_v$) has a slope of 1.48 and $R^2 = 0.63$. In this paper, we propose a computational algorithm that addresses a related question: 'Are wide vessels also long vessels?' within a species. In this paper, we use L_c and D_c to mean the vessel length and vessel diameter in a bin size class, respectively.

METHODS

Silicone rubber injection

Stem segments about 30–50 cm long were collected from two cottonwood hybrids: cv P38P38 (*Populus balsamifera* × *Populus simonii*) and cv. Northwest (*Populus deltoides* × *P. balsamifera*) and from seedlings of aspen (*Populus tremuloides* Michx). Hybrid clones were grown from cuttings and *P. tremuloides* from seeds in a greenhouse for 4 months, and were 1–2 m tall when harvested. Stem segments were injected with silicone rubber using the technique described in Sperry, Hacke & Wheeler (2005) and Wheeler *et al*. (2005). Briefly, silicone rubber was freshly mixed from liquid silicone and hardener in the ratio of 10:1 (10 g RTV141 part A plus 1 g RTV141 part B) (Rhodorsil RTV-141; Rhodia USA, Cranbury, NJ, USA; imported by Walco Materials, Escondido, CA, USA). Uvitex, a

Correspondence: M. T. Tyree. E-mail: Mel.Tyree@ales.ualberta.ca

fluorescent whitening agent (Ciba Uvitex OB; Ciba Specialty Chemicals, Tarrytown, NY, USA), was added to make the silicone visible under UV light. The Uvitex was dissolved in chloroform (1% w/w) and 10 drops added to the silicone mix (Hacke, Sperry & Field 2007).

Five stem segments per species were first flushed with 100 mM KCl solution filtered to 0.2 μm at 0.05 MPa for 30 min in order to remove air bubbles that would interfere with the injection of silicone rubber solution. After the water flush, the stems were injected with silicone at 0.05 MPa for 24 h, and then the silicone was allowed to cure (harden) for 3 more days at room temperature (22 °C) prior to sectioning. The cured stems were cross-sectioned at several distances (0.2, 0.5, 1.0, 1.5, 2.0, 3.0, 5.0 cm) from the injection surface, and photographs were taken for vessel diameter measurement and count as described below.

Vessel diameter measurements

Diameters of rubber-filled and, sometimes, non-rubber-filled vessel were measured as a function of distance away from the injection point. A microtome (Reichert-Jung 2030 Biocut; Leica, Heidelberg, Germany) was used to cut 30-mm-thick cross-sections from rubber-filled stems. These sections were mounted in water on a glass slide and placed on a microscope (Zeiss Axioskop 40; Carl Zeiss Microlmaging GmbH, Göttingen, Germany), and photographed with a digital camera (Infinity1-5C; Regent Instruments Inc, Quebec City, Canada) at 40× magnification under UV and visible light to make the rubber dye fluoresce brightly while still being able to see the walls. Then, image analysis software (Win CELL 2007; Regent Instruments Inc) was used to measure the diameter of every filled or unfilled vessel in three pie-shaped wedges in different (evenly distributed) directions around the cross-section. At least 1000 vessels were measured in one section, and the cross-sectional area of the wedges was recorded.

The diameter was computed from vessel cross-sectional area (A) for a circle of equal area $D = \sqrt{4A/\pi}$. Using the Microsoft Excel histogram function, the vessel diameters were divided into bin diameters (diameter size classes, D_c, of 10 μm width), and the counts in each diameter size class were used to compute frequency distributions, and probability density functions (PDFs) were fitted to these distributions.

We found that 'frequency distributions' of % vessels in different diameter size classes could be fitted with Weibull PDF:

$$f(x_b; \lambda, k) = \frac{k}{\lambda}\left(\frac{x_b}{\lambda}\right)^{(k-1)} \exp\left[-\left(\frac{x_b}{\lambda}\right)^k\right], \quad (1)$$

where k and λ are fitting constants, and x is the bin diameter increment defined as $x_b = \frac{D_c}{d_w}$, where d_w is the bin width (typically 5 μm), and D_c is the diameter at the centre of the vessel diameter size class, for example $D_c = 12.5$ μm for the vessel diameter size classes from 10 to 15 μm, and hence $x_b = 2.5$ for vessel diameter size classes of 10–15 μm.

Computational algorithm for vessel length

The normal computation algorithm is to count the number of vessels per unit cross-sectional area in pie-shaped wedges $N = n/$(cross-sectional area) and plot ln(N) versus distance from the injection surface (x) to compute λ_v. The exponential extension of vessel ends is given by

$$N = N_o \exp(\lambda_v x) \quad (2)$$

where N_o is the number of vessels filled at $x = 0$, and N is the number at $x > 0$ and λ_v is a fitting coefficient (a negative quantity for an exponential decay), hence a natural log transform plot can be used to estimate λ_v. As pointed out by Cohen, John Bennink & Tyree (2003) and Sperry *et al.* (2005), the second derivative of Eqn 2 gives the PDF:

$$P_x = x\lambda_v^2 \exp(\lambda_v x)\mathrm{d}x \quad (3)$$

In Eqn 3, P_x is the probability of vessels in the length interval dx. Cohen (personal communication) has determined that Eqn 3 is a gamma PDF with shape factor = 2, mode = $-1/\lambda$ and mean vessel length $\bar{L}_v = -2/\lambda_v$.

The modified computational algorithm assumed that vessels in a given size class maintain approximately constant diameter over their entire length. Vessel widths were divided into bins based on diameter size classes, and the counts in each size class (N_c) were used for the plots of ln(N_c) versus x. Size classes where N_c at $x = 0.2$ cm was less than 50 were excluded from analysis diameter.

Replication and statistical methods

Vessel counts in each diameter size class (N_c) were obtained on five replicate stems for each species at various distances, x, from the injection surface. Mean N_c ($\bar{N}_c$) and standard errors were used in plots of $\ln(\bar{N}_c)$ versus x from which slopes were obtained in each size class (λ_v in Eqn 2). The value of λ_v for each diameter size class (λ_c) was then used to compute the mean vessel length in that size class ($\bar{L}_c = -2/\lambda_c$). $\bar{L}_c$ was plotted versus the diameter size classes (D_c). Linear and two-parameter non-linear regressions of $\bar{L}_c$ versus D_c were obtained using SigmaPlot (version 11), and the resulting statistics were used to evaluate if trends were significantly different from zero slope.

RESULTS

The number of vessels filled with injected silicone rubber fell exponentially with distance from the injection surface as frequently found by others (data not shown, see Sperry *et al.* 2005). Vessel diameters were measured in filled and unfilled vessels at 2 cm from the injection surface, and turned into frequency histograms. Histograms were fitted to a Weibull PDF (Eqn 3). Two examples at 2 cm from the

injection point are shown in Fig. 1 for cottonwood clones P38P38 and Northwest. In all cases examined, the PDF was shifted to the right for filled versus unfilled vessels. From this, it follows that wide vessels tend to be long vessels.

Two examples of log-transformed vessel count with standard error bars are shown in Fig. 2. The slopes of these lines yielded λ_v from Eqn 2, and mean vessel diameter in each size class was computed from $\bar{L}_c = -2/\lambda_v$. Figure 3 shows plots of $\bar{L}_c$ versus diameter size class, D_c. Plots in Fig. 3 have non-zero slopes that are significantly different from zero. The computational methods and assumptions provide no theoretical guidance on the likely functional dependence of $\bar{L}_c$ on D_c. Plots appeared linear to slightly exponential, hence both linear and two-parameter exponential functions were fitted to see which had higher R^2 values. The regressions with the higher R^2 are reported. The slopes suggest that in all species, vessel length increases with vessel width, and that this dependence on width is more highly expressed in Northwest than in P38P38, and aspen is intermediate. The values of $\bar{L}_v$ and $\bar{D}_v$ computed by the traditional algorithm (Cohen *et al*. 2003; Sperry *et al*. 2005) fall within the range of $\bar{L}_c$ and D_c for each clone (stars in Fig. 3).

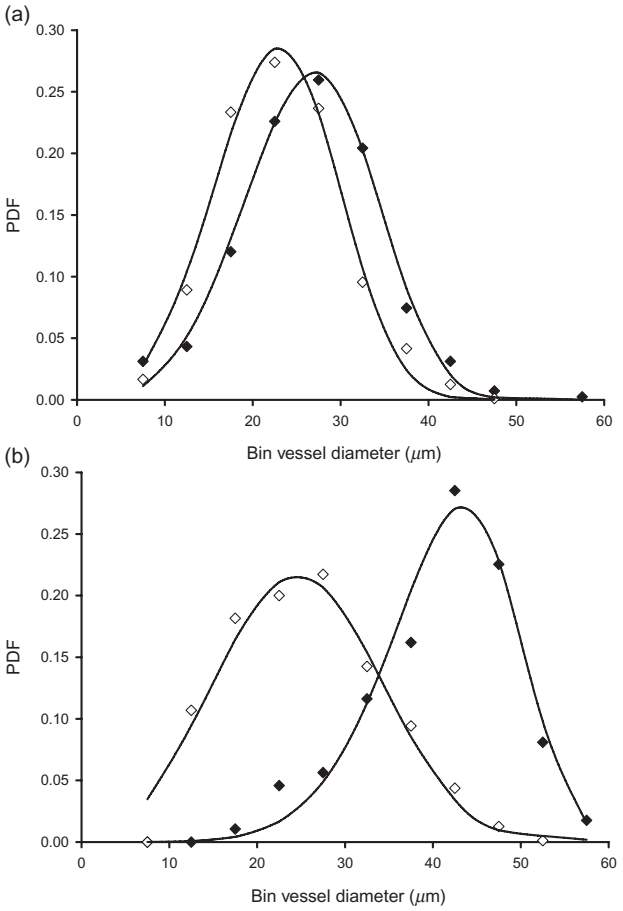

Figure 1. (a) Vessel diameter probability density functions (PDFs) of P38P38 hybrid cottonwood vessels filled (closed symbols) and unfilled (open symbols) with silicone rubber at 2 cm from the injection point. (b) Vessel diameter PDFs of Northwest hybrid cottonwood vessels filled (closed symbols) and unfilled (open symbols) with silicone rubber at 2 cm from the injection point.

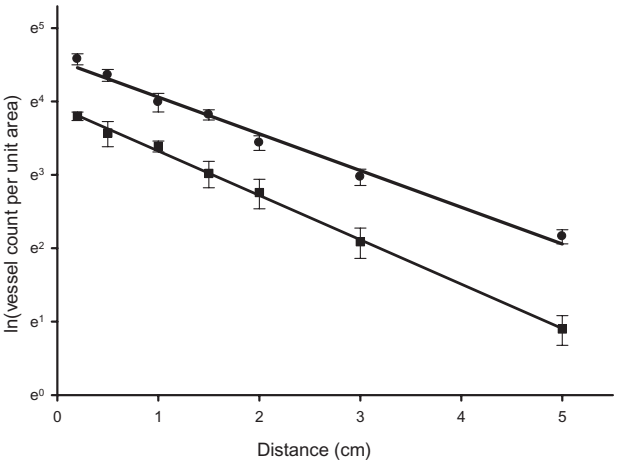

Figure 2. Two examples of natural log-transformed plots of vessel count per unit area in a diameter size class versus distance from the injection surface. Shown are means and standard error of counts in five stems for cottonwood clones Northwest (squares) and P38P38 (circles). The slopes of these lines are used to evaluate λ_v in Eqn 2 for a vessel diameter size class.

DISCUSSION

The algorithm used in this paper is based on the assumption that vessel diameters do not change much over their length. What proof is there that vessels maintain more or less constant width over their length?

In one published study of *Cedrela fissilis* stems, vessel size and location had been measured in serial sections and recorded by the cinematographic method. The published scale drawings showed plots of vessel width and position. Careful examination of the plot reveals that narrow vessels remain narrow over their entire length in the analysed block of wood, and wide vessels remain wide over their length (see fig. 2.2 in Tyree & Zimmermann 2002).

If wide vessels are long vessels, then we would expect the PDF of rubber-filled vessels to contain a higher frequency of wide vessels than in the PDF of unfilled vessels when evaluated at a non-zero distance from the injection surface. This is confirmed by our data in Fig. 2 where we evaluated the PDFs of filled and unfilled vessels at 2 cm from the injection surface. Qualitatively, similar curves (not shown) were evaluated at other distances where wide vessels were more commonly rubber filled. In addition, if vessels of any diameter can be any random length, then the slopes of the plots of $\ln(N_c)$ versus x should be the same for any diameter size class. However, the contrary is true as evidenced by the strong dependence of $\bar{L}_c$ on vessel width (Fig. 3).

The algorithm used in this paper provides an indication that wide vessels tend to be long vessels in cottonwood hybrids and aspen. This information has some useful implications provided the pit area hypothesis is true. According to the pit area hypothesis, the vulnerability of a vessel to

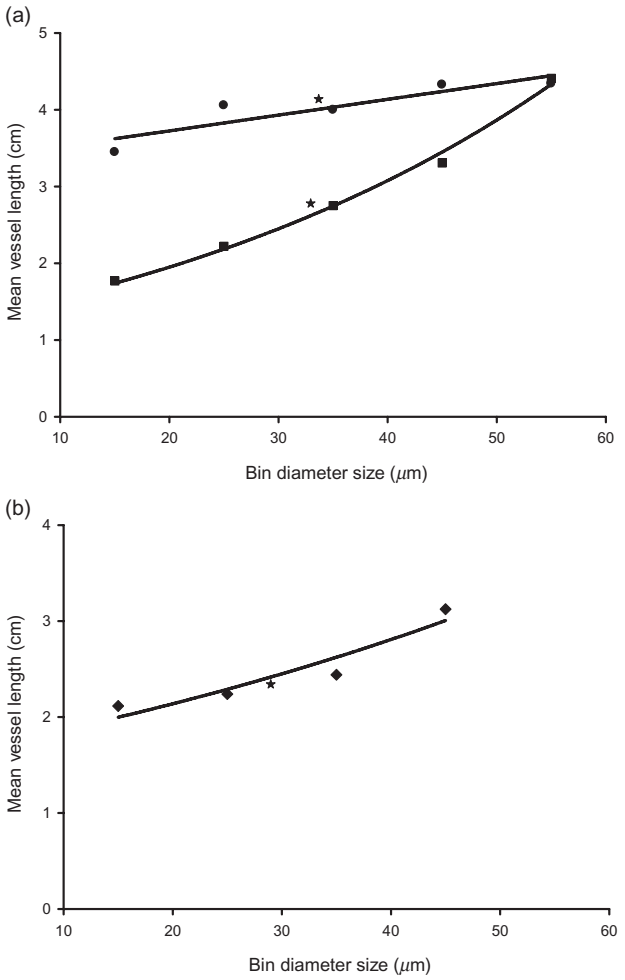

Figure 3. (a) Mean vessel length in a diameter size class, $\bar{L}_c$ versus vessel diameter size class (D_c) is shown for two cottonwood clones: Northwest (squares) and P38P38 (circles). The regressions are: Northwest: $\bar{L}_c = 1.235\ \exp(0.0228 D_c)$ ($R^2 = 0.997$ SE of slope = ± 0.0011 $P = 0.0003$) and P38P38: $\bar{L}_c = 0.0206\ D_c + 3.314$ ($R^2 = 0.804$ SE of slope = ± 0.006 $P = 0.04$). The star points are at the coordinates for $\bar{L}_v$ and $\bar{D}_v$ for each clone. (b) Similar data for aspen. Only four diameter bin sizes are shown because the range of diameters was less than in (a). Regression $\bar{L}_c = 1.681\ \exp(0.0126 D_c)$ ($R^2 = 0.890$ SE of slope = ± 0.0033 $P = 0.05$).

embolism increases with the surface area of all pits in that vessel. Our data lend additional support to the notion (Wheeler *et al*. 2005) that there is a trade-off between vessel efficiency for water transport and vulnerability to drought-induced xylem embolism. The Hagen–Poiseuille equations predict that hydraulic conductivity should increase with D^4, and long vessels will have less end wall resistance because of increased surface area for pit membranes. Both of these factors make wide and long vessels very efficient transporters of water. The trade-off between efficiency and vulnerability to cavitation might drive a shift in vessel length of wide vessels away from the optimum value for hydraulic efficiency within a species.

The theoretical dependency of L versus D for optimized vessel design has been discussed at length (Lancashire & Ennos 2002, Wheeler *et al*. 2005; Hacke *et al*. 2006), and is postulated to follow eqn 6 in Hacke *et al*. (2006). Full discussion of this equation is beyond the scope of this paper, but the form of the equation is:

$$L = 0.125\left(\frac{F \times r_p}{\eta \times F_p \times F_L}\right)^{1/2} D^{3/2} \quad (4)$$

where F is the ratio of the lumen-to-wall hydraulic resistance, r_p is the pit membrane resistance, η is the viscosity of water, F_p is the pit fraction (total pit area per area of vessel wall) and F_L is the length fraction (length of vessel in contact with adjacent vessels to vessel length). If the half-power term in Eqn 4 is constant, then a plot of $\log(L)$ versus $\log(D)$ should have a slope of 1.5. Given that there are so many parameters in the half power term in brackets that might scale with D, it is surprising that a plot of $\log(L)$ versus $\log(D)$ had a slope of 1.48 in Hacke *et al*. (2006). Our values from *Populus* species show a much lower slope when a regression of the form $L = aD^b$ is performed. For P38P38, NW and aspen, the value of b, which is the slope of the log–log transform, equals 0.17, 0.77 and 0.36, respectively.

All that can be said at this point is that the computational algorithm used in this paper produces a much smaller scaling relationship between vessel length and vessel diameter within a species (cottonwood hybrid and aspen) than found by Hacke *et al*. (2006) between species. If Eqn 4 applies within a species, then the difference could be accounted for by saying: (1) that the parameters in the half power term do scale with D within a species; (2) vessel diameter and length within a species do not follow an optimized hydraulic pattern within a species for reasons of safety; (3) the new assumption in the computational algorithm (that vessel diameter is constant along the length of a vessel) is qualitatively correct, but not quantitatively correct; or (4) a combination of (1) through (3) is true.

ACKNOWLEDGMENTS

This research was made possible by research grants from the Canadian Forest Service, Natural Sciences and Engineering Research Council Discovery Grant, Alberta Forestry Research Institute, Alberta Ingenuity Equipment Grant and endowment funds from the Department of Renewable Resources, University of Alberta. M.T.T. wishes to thank the United States Forest Service for salary support while working at the University of Alberta, which made this study possible. J.C. wishes to thank the China Scholarship Council for travel costs to Canada, and thanks to Northwest A&F University for granting leave from teaching duties to work at the University of Alberta as a visiting professor for 2 years. We thank Dr Barb Thomas and Alberta-Pacific Forest Industries Inc for providing cutting of the cottonwood clones used in this study.

REFERENCES

Cohen S., John Bennink J.P. & Tyree M.T. (2003) Air method measurements of apple vessel length distributions with improved apparatus and theory. *Journal of Experimental Botany* **54,** 1889–1897.

Ewers F.W. & Fisher J.B. (1989) Techniques for measuring vessel lengths and diameters in stems of woody plants. *American Journal of Botany* **76,** 645–656.

Ewers F.W., Fisher J.B. & Chiu S.-T. (1990) A survey of vessel dimensions in stems of tropical lianas and other growth forms. *Oecologia* **84,** 544–552.

Grenidge K.N.H. (1952) An approach to the study of vessel length in hardwood species. *American Journal of Botany* **39,** 570–574.

Hacke U.G., Sperry J.S., Wheeler J.K. & Castro L. (2006) Scaling of angiosperm xylem structure with safety and efficiency. *Tree Physiology* **26,** 689–701.

Hacke U.G., Sperry J.S. & Field T.S. (2007) Water transport in vesselless angiosperms: conducting efficiency and cavitation safety. *International Journal of Plant Sciences* **168,** 1113–1126.

Lancashire J.R. & Ennos A.R. (2002) Modeling the hydrodynamic resistance of bordered pits. *Journal of Experimental Botany.* **53,** 1485–1493.

Loepfe L., Martinez-Vilalta J., Piñol J. & Mencuccini M. (2007) The relevance of xylem network structure for plant hydraulic efficiency and safety. *Journal of Theoretical Biology* **247,** 788–803.

Scholander P.F. (1958) The rise of sap in lianas. In *The Physiology of Forest Trees* (ed. K.V. Thimann), pp. 3–17. Ronald Press, New York, NY, USA.

Skene D.S. & Balodis V. (1968) A study of vessel length on *Eucalyptus obliqua* L'herit. *Journal of Experimental Botany* **19,** 825–830.

Sperry J.S., Hacke U.G. & Wheeler J.K. (2005) Comparative analysis of end wall resistance in xylem conduits. *Plant, Cell & Environment* **28,** 456–465.

Tyree M.T. (1993) Theory of vessel-length determination: the problem of nonrandom vessel ends. *Canadian Journal of Botany* **71,** 297–302.

Tyree M.T. & Zimmermann M.H. (2002) *Xylem Structure and the Ascent of Sap* 2nd edn, Springer, Berlin, Germany.

Wheeler J.K., Sperry J.S., Hacke U.G. & Hoang N. (2005) Intervessel pitting and cavitation in woody *Rosaceae* and other vesselled plants: a basis for safety versus efficiency trade-off in xylem transport. *Plant, Cell & Environment* **28,** 800–812.

Zimmermann M.H. (1971) *Dicotyledonous Wood Structure Made Apparent by Sequential Sections (Film E 1735)*. Institut für den wissenschaftlichen Film, Göttingen, Germany.

Zimmermann M.H. (1978) Vessel ends and the disruption of water flow in plants. *Phytopathology* **68,** 253–255.

Zimmermann M.H. & Jeje A.A. (1981) Vessel-length distribution in stems of some American woody plants. *Canadian Journal of Botany* **59,** 1882–1892.

Received 21 January 2010; accepted for publication 12 February 2010